

Endoscopic, rapid near-infrared optical tomography

Daqing Piao, Hao Xie, Weili Zhang, and Jerzy S. Krasinski

School of Electrical & Computer Engineering, Oklahoma State University, Stillwater, Oklahoma

Guolong Zhang

Department of Animal Science, Oklahoma State University, Stillwater, Oklahoma

Hamid Dehghani

Department of Physics, University of Exeter, Exeter, UK

Brian W. Pogue

Thayer School of Engineering, Dartmouth College, Hanover, New Hampshire

Received May 23, 2006; revised June 27, 2006; accepted July 11, 2006;
posted July 11, 2006 (Doc. ID 71316); published September 11, 2006

This is believed to be the first demonstration of near-infrared (NIR) optical tomography employed at the endoscope scale and at a rapid sampling speed that allows translation to *in vivo* use. A spread-spectral-encoding technique based on a broadband light source and linear-to-circular fiber bundling was used to provide endoscopic probing of many source-detector fibers for tomography as well as parallel sampling of all source-detector pairs for rapid imaging. Endoscopic NIR tomography at an 8 Hz frame rate was achieved in phantoms and tissue specimens with a 12 mm probe housing eight sources and eight detectors. This novel approach provides the key feasibility studies to allow this blood-based contrast imaging technology to be attempted in detection of cancer in internal organs via endoscopic interrogation. © 2006 Optical Society of America

OCIS codes: 170.6960, 170.2150, 170.3880, 120.3890.

The attenuation of near-infrared (NIR) light between blood and parenchymal tissue has considerably high contrast owing to the hemoglobin attenuation in blood. The hypervascularity in tumors produces an elevated hemoglobin content and hence high intrinsic optical contrast between tumor and normal tissues. This high tumor-tissue contrast, reinforced by the concept of noninvasive optical measurement, has made NIR optical tomography an interesting technique for imaging the vasculature-based tumour functionality. Although there is high NIR contrast, unfortunately noninvasive cancer imaging by NIR has been restricted to specific organs that can be transilluminated externally. NIR tomographic breast imaging is employed because the tissue can be easily interrogated by direct contact with NIR sources-detectors. Breast imaging validation studies have shown high sensitivity and specificity based upon vasculature differences and multiple clinical trials are ongoing.¹⁻⁴ The hypervascularity present in tumors of other internal organs such as the prostate, colon, and rectum likely has similar high tumor-tissue contrast in NIR imaging, but the key factor in attempting these studies is the development of an appropriate applicator array. For the prostate, studies have focused on NIR measurement of optical properties in experimental prostate tumors *in vivo*⁵ and human prostate,⁶ as well as surface measurements of implanted prostate tumors to quantify the hemodynamic changes.⁷ All these studies have demonstrated that physical principles of NIR measurements can be used on internal organ tissues; however, these mea-

surements are either nonlocalized or limited to the superficial area. If NIR measurements of internal organs can be performed in tomographic mode, it will provide two-dimensional contrast mapping at depths up to a few centimeters below the surface, hence providing new contrast information on a distance scale similar to ultrasound. NIR optical tomography of prostate *in situ* requires an endoscopic probe geometry. The size of this probe must be on the millimeter to centimeter scale, similar to what has been developed for tomography of finger joints,⁸ where there is no difficulty of placing the fibers exterior to the array. For endoscopic NIR tomography, however, many fibers have to be housed in the internal space of a very small probe. This presents a major technical challenge for endoscopic NIR optical tomography. The second challenge is the rapid imaging requirement for this technique to be clinically applicable. It is well known in NIR tomography that rapid imaging is difficult, for there exist only a few systems of sampling faster than 1 Hz.^{9,10}

The work presented in this Letter is, to the best of our knowledge, the first demonstration that NIR optical tomography can be performed in endoscopic mode and that endoscopic NIR tomography can be implemented at rapid sampling speed. This technique is based on a novel approach of spread-spectral-encoding of a broadband light source in combination with linear-to-circular fiber bundling, by which multiple source-detector fibers can be enclosed in a probe for endoscopic NIR tomography and parallel source delivery can be realized for rapid sampling

of tomographic data.¹⁰ In this Letter we report on endoscopic 8 Hz NIR tomography of phantom and animal specimens from a 12 mm diameter probe housing eight source fibers and eight detector fibers.

The schematic diagram of the endoscopic, rapid NIR optical tomography system is illustrated in Fig. 1. A broadband light is dispersed by a grating positioned at the focal plane of a planar-convex lens, and the collimated beam strip is incident upon a linear fiber bundle located at the other focal plane of the lens. The light coupled to each fiber has a wavelength separation [Fig. 2(a)], hence each fiber functions as a source that is spectrally encoded and can be delivered to the tissue in parallel. A spectrometer is then used to spectrally decode the signals, allowing concurrent sampling of entire source-detector pairs by CCD camera. This parallel sampling principle is similar to the recently introduced spectral-encoding method based upon laser diodes (LDs) that led to the first video-rate NIR optical tomography.^{10,11} The LD-based configuration, however, is difficult for endoscopic probing owing to the bulky light coupling from many LDs to the fibers. This previous system also used individual temperature and current controllers to tune each LD to maintain a different emission wavelength, which becomes cumbersome and potentially problematic when many LDs are needed. The use of a broadband source by spread-spectral-encoding preserves the feature of parallel sampling required for rapid imaging and suffices for the need of an endoscopic probe. The linear fiber bundle for source coupling can be made of bare fibers or thin-coating fibers, thus many fibers can be housed inside the endoscope probe by rearranging the fibers circularly. A coated cone prism can then be used for 90° circumferential light deflection. The light detection is conveyed by another circular fiber array that is concen-

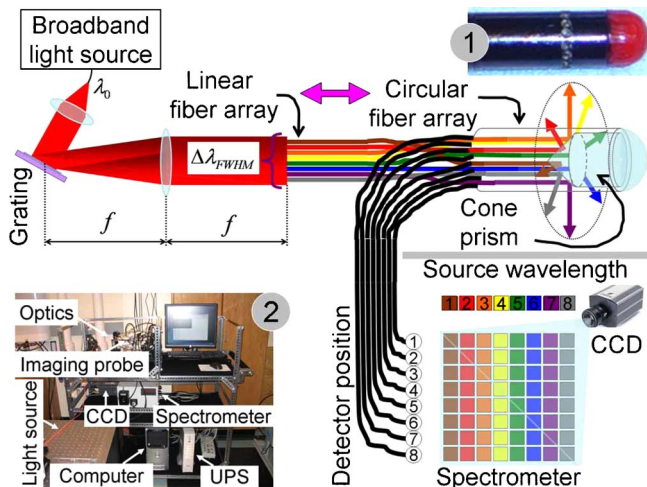


Fig. 1. (Color online) Schematic of the endoscopic, rapid NIR optical tomography system. The broadband light was dispersed by a grating and collimated upon a linear fiber array. The fiber array delivered spectral-encoded sources to the probe where the fibers were rearranged circularly. A coated cone prism was used for 90° deflection. The detected light was separated by a spectrometer, allowing simultaneous sampling of all source-detector pairs. Insets 1 and 2 are photographs of the 12 mm diameter probe and the system, respectively.

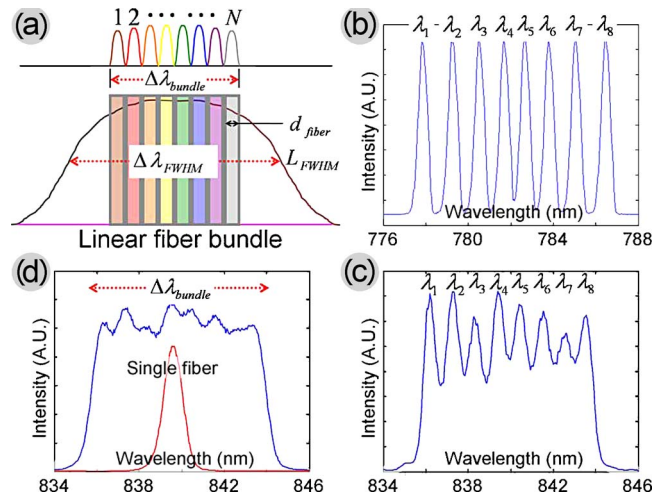


Fig. 2. (Color online) Principle of spread-spectral-encoding: (a) coupling of dispersed broadband light to a linear fiber bundle to obtain spectral encoding, (b) spectral coupling profile in the previous LD-based system, (c) spectral profiles coupled to the linear fiber bundle as well as single fiber, (d) spectral profile after deconvolution.

tric to and interspersed with the source array, which at the other end is also linearly aligned for spectrometer coupling. This design integrates the endoscopic probe with the rapid sampling approach for spectrally encoded NIR optical tomography.

The dimension of the beam strip at the fiber facet plane is $L_{FWHM} = f \Delta \lambda_{FWHM} / \{p [1 - (\lambda_0/p - \sin \alpha)^2]^{1/2}\}$, where f is the focal length, $\Delta \lambda_{FWHM}$ is the source spectral bandwidth, λ_0 is the center wavelength, p is the grating period, and α is the beam incident angle with respect to the grating axis. For N bare fibers aligned side by side, as shown in Fig. 2(a), the spectral band coupled to the fiber bundle is $\Delta \lambda_{bundle} = \Delta \lambda_{FWHM} N d_{fiber} / L_{FWHM}$, where d_{fiber} is the fiber diameter. The grating was 1200 grooves/mm, the lens had $f=200$ mm, and the fiber bundle was fabricated with eight 800 μm bare fibers. When a 840 nm superluminescent diode of 40 nm bandwidth and 20 mW output power was used, 8.3 nm was coupled to the fiber bundle. In comparison with the previous system [Fig. 2(b) is a reproduction of Fig. 2(a) in Ref. 10], this system coupled a narrower bandwidth that was beneficial for the maintenance of relatively uniform absorption among sources. However, the coupled spectrum appeared as a spread profile. To quantify the coupling to the individual fibers, the spread profile was deconvolved with the measured single-fiber-coupling profile [the Gaussian-shaped curve in Fig. 2(c)]. The profile after deconvolution is shown in Fig. 2(d), where each fiber is well delineated such that the data manipulation methods used for the previous study could be applied. The uneven coupling that appeared was due to fabrication error, and it was normalized before reconstruction.¹¹

The NIR probe housed the eight source-coupling fibers and eight additional detection fibers, all 800 μm in diameter. A 10 mm cone prism was used. The cone prism and the fiber-holding ferrule were mounted together by a 12 mm diameter black sleeve, on the surface of which sixteen 1.5 mm holes were drilled and

sealed with transparent optical epoxy to serve as the aperture. A sampling speed of 8 Hz was reached by use of the superluminescent diode source.

Image reconstruction was performed with NIRFAST¹² by implementing a hollow-centered circular mesh to account for the nonconventional imaging geometry in endoscopic NIR tomography. For the 12 mm probe, the minimum source–detector distance along the peripheral was 2.4 mm. This short distance might have introduced reconstruction error since NIRFAST is based on the diffusion approximation; nevertheless, the preliminary results with phantom and animal tissue were satisfactory when absorption contrasts were localized.

Figure 3 shows two imaging examples. In Fig. 3(a) the probe was placed in 1% Intralipid solution, giving an absorption coefficient of 0.002 mm^{-1} , and a 6.35 mm polycarbonate rod was moved manually along the surface of the probe. The movement was between the 12 o'clock and 6 o'clock positions with a cycling time of approximately 1 s when eight frames were acquired. The reconstruction field of view was set to an inner diameter of 12 mm and an outer diameter of 36 mm. The localizations of the occlusion with 1/8 s apart were excellent, except for weak amplitude in the 0.25 s frame. The images shown in Fig. 3(b) demonstrate transrectal NIR tomography from a freshly excised normal chicken rectum. The rectum wall was 1–2 mm thick and was quite uniform in terms of absorption. To generate absorption contrast, 0.3 cc of 0.2% diluted India ink was injected into the rectum wall [dashed circle in Fig. 3(b)]. The entire rectum specimen was then enclosed by the fallopian tube and other smooth chicken tissues to simulate a homogeneous background medium in depth. The inserted NIR probe was pushed and pulled manually across the ink-injection region. The single push-pulling cycle took slightly over 2 s, and four frames 1.125 s apart covering two cycles were displayed. The

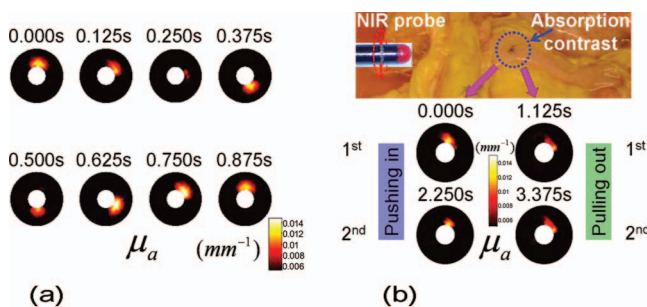


Fig. 3. Examples of endoscopic, 8 Hz NIR tomography: (a) Imaging of a dynamic object in 1% Intralipid solution. The occlusion was a 6.35 mm polycarbonate rod moved manually from 12 o'clock to 6 o'clock clockwise and counterclockwise from 6 o'clock back to 12 o'clock. The movement cycle took approximately 1 s. (b) Imaging of chicken rectum *ex vivo* with 0.3 cc of 0.2% India ink injected into the rectum wall. The inserted probe was push-pulled manually across the ink-injection region in a cycle of approximately 2 s.

images corresponding to the two push-in cycles are quite similar, and the two pull-out images are almost identical to each other. The difference between the push-in and pull-out images may be related to the location mismatch within the ink region.

In summary, a novel technique of endoscopic, rapid NIR optical tomography has been demonstrated. The spread-spectral-encoding based on a broadband light source was implemented for parallel light delivery to achieve rapid sampling, and linear-to-circular fiber bundling ensured the housing of many source–detector fibers in the probe for endoscopic tomography. Endoscopic NIR optical tomography may represent a new paradigm of tomographic cancer imaging in internal organs with high intrinsic optical contrast. The accurate light transport models for endoscopic NIR optical tomography may also be a significant topic to investigate in the future.

The authors acknowledge the initial support by National Institutes of Health through grant 1R21CA100984-01A1 and the start-up fund from the College of Engineering, Architecture and Technology of Oklahoma State University. The discussion with Shudong Jiang is also appreciated. D. Piao's e-mail address is daqing.piao@okstate.edu.

References

1. M. A. Franceschini, K. T. Moesta, S. Fantini, G. Gaida, E. Gratton, H. Jess, W. W. Mantulin, M. Seeber, P. M. Schlag, and M. Kaschke, *Proc. Natl. Acad. Sci. U.S.A.* **94**, 6468 (1997).
2. B. J. Tromberg, O. Coquoz, J. B. Fishkin, T. Pham, E. R. Anderson, J. Butler, M. Cahn, J. D. Gross, V. Venugopalan, and D. Pham, *Philos. Trans. R. Soc. London, Ser. B* **352**, 661 (1997).
3. B. W. Pogue, S. P. Poplack, T. O. McBride, W. A. Wells, K. S. Osterman, U. L. Osterberg, and K. D. Paulsen, *Radiology* **218**, 261 (2001).
4. V. Ntziachristos, A. G. Yodh, M. D. Schnall, and B. Chance, *Neoplasia* **4**, 347 (2002).
5. M. R. Arnfield, J. D. Chapman, J. Tulip, M. C. Fenning, and M. S. McPhee, *Photochem. Photobiol.* **57**, 306 (1993).
6. T. Zhu, A. Dimofte, J. C. Finlay, D. Stripp, T. Busch, J. Miles, R. Whittington, S. B. Malkowicz, Z. Tochner, E. Glatstein, and S. M. Hahn, *Phys. Plasmas* **81**, 96 (2005).
7. M. Goel, H. Radhakrishnan, and H. Liu, paper SH10 presented at the OSA Biomedical Topical Meetings, Fort Lauderdale, Florida, March 19–22, 2006.
8. A. K. Scheel, M. Backhaus, A. D. Klose, B. Moa-Anderson, U. Netz, K. G. Hermann, J. Beuthan, G. A. Müller, G. R. Burmester, and A. H. Hielscher, *Ann. Rheum. Dis.* **64**, 239 (2005).
9. C. H. Schmitz, M. Löcker, J. M. Lasker, A. H. Hielscher, and R. L. Barbour, *Rev. Sci. Instrum.* **73**, 429 (2002).
10. D. Piao, S. Jiang, S. Srinivasan, H. Dehghani, and B. W. Pogue, *Opt. Lett.* **30**, 2593 (2005).
11. D. Piao, H. Dehghani, S. Jiang, S. Srinivasan, and B. W. Pogue, *Rev. Sci. Instrum.* **76**, 124301 (2005).
12. <http://www-nml.dartmouth.edu/nir/downloads.html>.